Geomorphometry of Normal Faults: Abyssal Hills and Continental Rifts

Peter L. Guth
Department of Oceanography
United States Naval Academy
Annapolis, MD 21402 USA
pguth@usna.edu

Abstract—**Normal faults in rifting environments create scarps with 10s to 100s of meters of relief, with strikes perpendicular to the spreading direction. Medium scale digital topography, with elevation spacing of 30-100 m, captures these features and allows extraction of the fault scarp orientations and relief. Digital elevation models like SRTM and ASTER GDEM cover the entire land surface at this scale, and significant underwater bathymetry exists, especially over mid-ocean ridges. Statistical techniques can identify fault scarps in these environments.**

I.   INTRODUCTION

Gilbert [1] first recognized the importance of normal faulting in creating horst and graben topography in the Basin and Range province of the western United States. A century later, Macdonald and others [2] recognized abyssal hills formed by normal faulting and volcanism as the most common geomorphic feature on earth, although obscured by several km of water.

Table 1 shows the three regions discussed in this paper. The DEMs come from the recently released 1" SRTM data set and the GMRT bathymetry [3], with resolution to capture fault scarps representing multiple faulting events. Plate motions from the MORVEL model [4] show that the Afar region, a type example for continental rifting [5], lies about 200 km south of a very slow active ridge in the Red Sea. The Atlantis Massif, one of the best studied oceanic cores complexes [6], also occurs on a very slow spreading ridge segment. The area on the East Pacific Rise has one of the fastest recorded spreading rates. Figure 1 shows the three areas, with earthquake focal mechanisms [7] shown for the two slow spreading areas. The East Pacific Rise has essentially no focal mechanisms with normal faulting in the global CMT database [7], but the strike slip faults on the transforms bounding this segment have one focal plane that parallels the MORVEL model spreading direction [4]. The bathymetric data sets [3] show significant void areas due to the difficulty and cost of guaranteeing complete coverage, but are complete enough to characterize the morphology of the abyssal hills.

TABLE I.   DATA SETS ANALYZED

Location	DEM	DEM Grid Size	Full Rate (mm/yr)	Plate Spreading
Afar Triangle	SRTM	1", ~30 m	18.9	54˚
Atlantis Massif	GMRT	~2",~ 53 m	22.3	102˚
East Pacific Rise	GMRT	~2", ~58 m	141.7	104˚

II.   FAULT SCARP CHARACTERISTICS

A normal fault plane, and the resulting fault scarp, can be defined by the dip and strike, or by its dip and dip direction. The dip and dip direction provide the least ambiguity, and correspond directly with the slope and aspect direction computed in standard GIS operations.

The two focal mechanisms for the normal faults in the Afar region and Atlantis Massif generally have the same strike, and dip 30-60˚ in opposite directions. Typically conjugate faults will develop with both orientations, but the dip at the surface may not equal the dip of the fault plane at the earthquake focus, and erosion might reduce the dip of the fault plane [8]. Fig. 2 shows profiles across the fault scarps in the three regions.

Fig. 3 shows the distribution of aspect for selected slope categories for two of the data sets. For the SRTM data from the Afar region, the overall data set and the flatter categories show a large overabundance of aspects in the 8 principal directions, a result of the quantization resulting from the integer resolution of the elevation data. While the gridded bathymetry may be no more accurate than the SRTM data, the floating point elevations smooth the aspect distribution. Both distributions show a strong tendency for the aspects to match the plate spreading direction. The East Pacific Rise data show a number of orthogonal aspects

for the slopes above 30%, which correspond with the conical volcanoes that occur in lines perpendicular to the ridge.
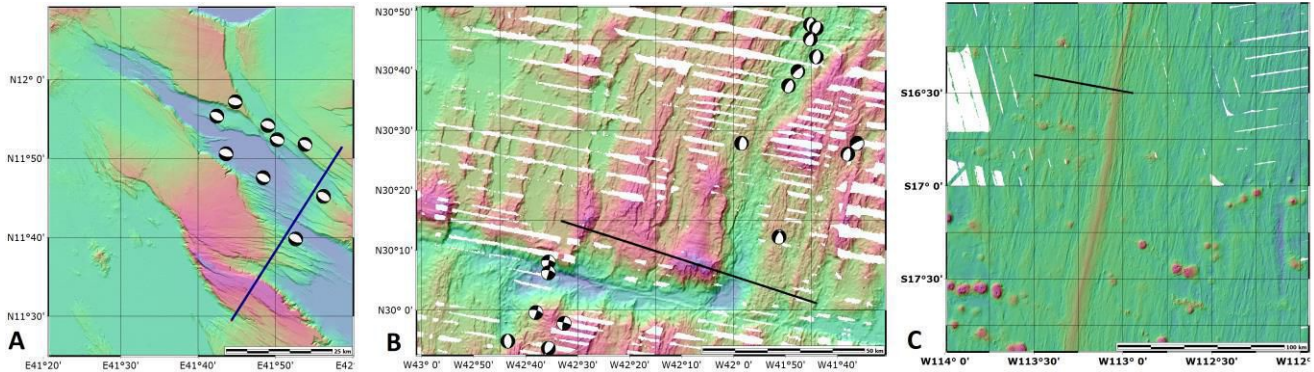

Figure 1.   Normal faults from Afar Triangle (A), Atlantis Massif on the Mid Atlantic Ridge (B), East Pacific Rise south of the Garrett Fracture Zone (C).
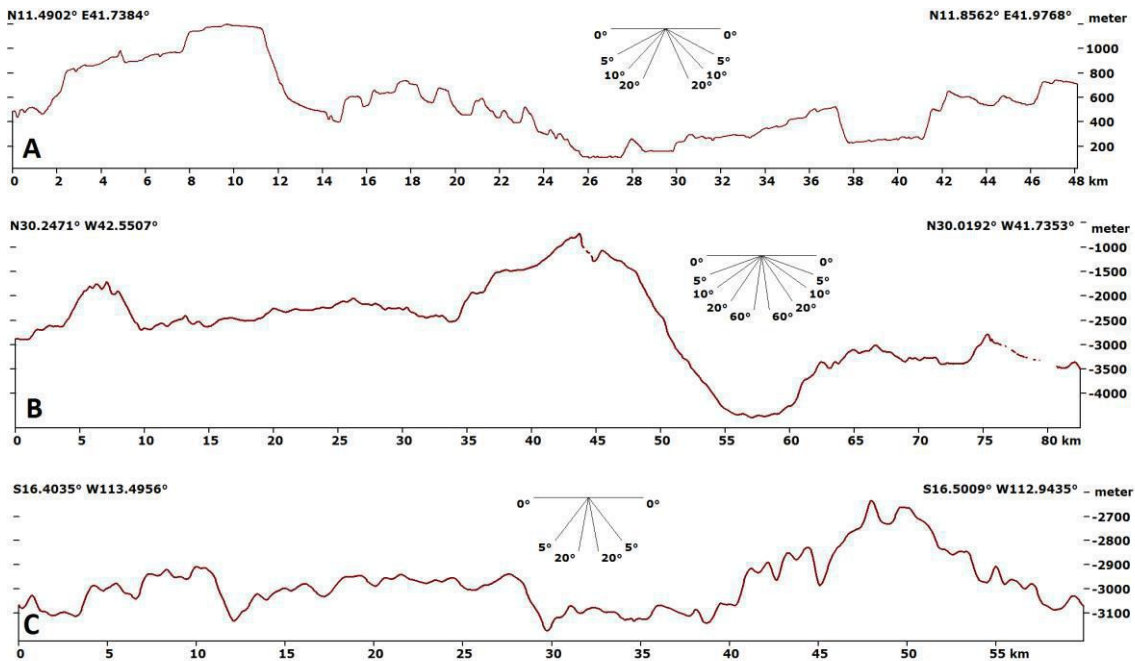

Figure 2.   Topographic profiles from Afar Triangle (A, vertical exaggeration 6 times), Atlantis Massif on the Mid Atlantic Ridge (B, vertical exaggeration 4 times, with ridge axis at 57 km), and East Pacific Rise south of the Garrett Fracture Zone (C, vertical exaggeration 15 times, with ridge axis at 50 km).

Fig. 3 shows the topographic fabric [9,10], with vector overlays that show the strength of the fabric with the vector lengths, and the orientation. The rose diagrams show the fabric perpendicular to the aspect directions in Fig. 3, and parallel to the strike of the fault planes. The fabric calculates an average for a region (500 m in Afar, 750 m in the bathymetric data due to the larger grid spacing), and excludes flat regions and those with no significant trend, and the rose diagrams show a strong concentration perpendicular to the extension direction. The rose diagrams in Fig. 4 have only a small fraction of the number of points in the aspect distributions in Fig.3, and the operation of computing area averages accentuates the regional trends.

Exceptions to the regional fabric orientation occur where secondary processes alter the topography. On the Mid Atlantic Ridge (Fig. 4B), the Atlantis Fracture Zone reorients the topography to an east-west trend, which also happens on the large

corrugations of the domal core complex. On the East Pacific Rise (Fig. 4C), domal volcanoes also deflect the linear pattern of abyssal hills.
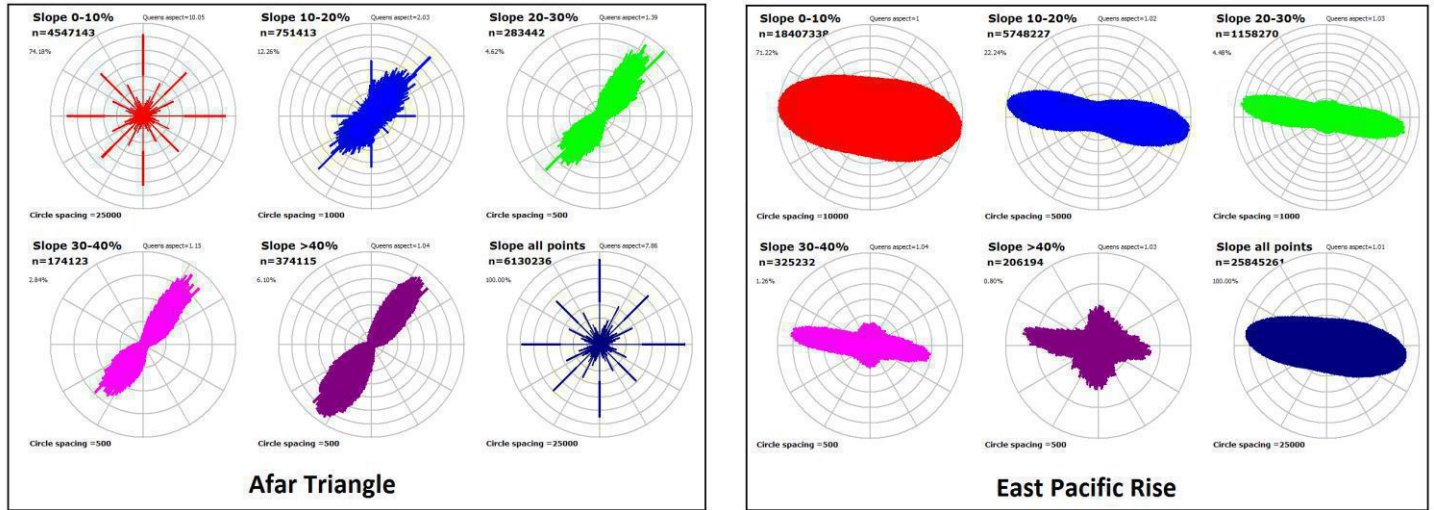

Figure 3. Aspect directions by slope category for the Afar Triangle and East Pacific Rise.
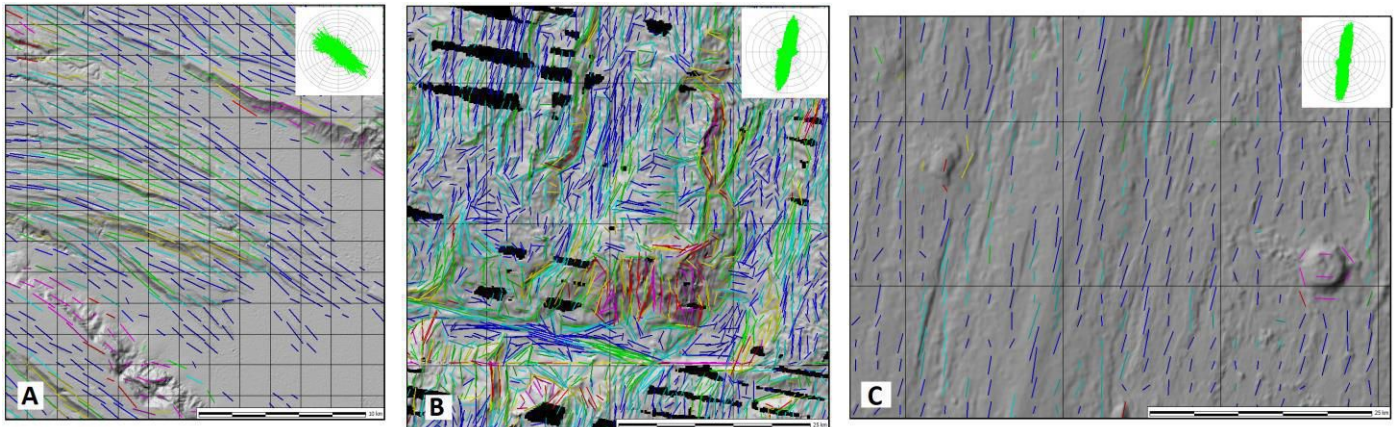

Figure 4. Topographic fabric, colored by local relief, for portions of the data sets covering the Afar Triangle (A), Atlantis Massif on the Mid Atlantic Ridge (B), and East Pacific Rise south of the Garrett Fracture Zone (C). Insets show distribution of fabric for the entire data set.

Figure 4 shows the relief in the regions used to define the topographic fabric. High values of relief distinguish the transform fault valley, core complex edifice, and submarine volcanoes from typical abyssal hills. Fig. 5 shows identification of likely fault scarps, using aspect and slope, or just the steepest slopes.

III. CONCLUSION AND FUTURE WORK

This analysis used medium scale topography. The orientation of the terrain fabric matches the fault planes inferred from plate tectonic models, and earthquake focal mechanisms. Aspect distributions reflect the fault scarps, and the combination of slope and aspect can identify likely scarps.

With the exploding availability of lidar DEMs with typical resolution of 1 m, the techniques will be applied and compared to other work [e.g.11] in the terrestrial realm; comparable bathymetric data sets remain beyond widespread accessibility. We will also work to create fault scarp objects, and look to model the changes in scarps as they transfer motion to other faults along strike.
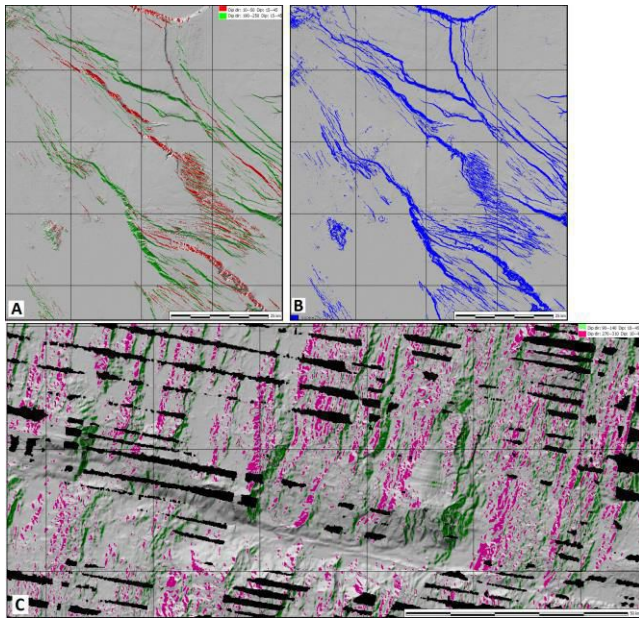
Figure 5.   (A). NE-dipping (red) and SW-dipping (green) surfaces in Afar defined by slope and dip direction. (B) Steep surface in Afar. (C) E-dipping (green) and W-dipping (red) surfaces along the Atlantis Fracture Zone.

REFERENCES

[1]   Gilbert, G.K., 1872, "Report of G.K. Gilbert, Geological Assistant, in Wheeler, G.M., Preliminary Report of Explorations Principally in Nevada and Arizona, U.S. Army Corps of Engineers, p.93-96.

[2]   Macdonald, K.C., Fox, P.J., Alexander, R.T., Pockalny, R., and Gente, P., 1996, Volcanic growth faults and the origin of Pacific abyssal hills: Nature vol. 380, p.125-129. doi:10.1038/380125a0.

[3]   Ryan, W.B.F., S.M. Carbotte, J.O. Coplan, S. O'Hara, A. Melkonian, R. Arko, R.A. Weissel, V. Ferrini, A. Goodwillie, F. Nitsche, J. Bonczkowski, and R. Zemsky, 2009. "Global Multi-Resolution Topography synthesis", Geochem. Geophys. Geosyst., 10, Q03014, doi: 10.1029/2008GC002332.

[4]   DeMets, C., Gordon, R. G., and Argus, D. F., 2010. "Geologically current plate motions", Geophysical Journal International, v. 181, no. 1, p. 1-80, doi: 10.1111/j.1365-246X.2009.04491.x.

[5]   Morton, W. H., and R. Black, 1975. "Crustal attenuation in Afar." Afar Depression of Ethiopia, A. Pilger and A. Rosier, eds., Inter-Union Commiss. Geodyn., Sci. Rep 14.

[6]   Whitney, D.L, C. Teyssier, P. Rey, and W. R. Buck, 2013, Continental and oceanic core complexes: Geological Society of America Bulletin, v. 125, no. 3-4, p. 273-298, doi:10.1130/B30754.1

[7]   Ekström, G., M. Nettles, and A. M. Dziewonski, 2012. "The global CMT project 2004-2010: Centroid-moment tensors for 13,017 earthquakes", Phys. Earth Planet. Inter., 200-201, 1-9, doi:10.1016/j.pepi.2012.04.002

[8]   Hilley, George E., J. R. Arrowsmith, and Lee Amoroso, 2001. "Interaction between Normal Faults and Fractures and Fault Scarp Morphology." Geophysical Research Letters 28, no. 19 , p. 3777-3780.

[9]   Guth, P.L., 2003, Eigenvector analysis of digital elevation models in a GIS: Geomorphometry and quality control: in Evans, I.S., Dikau, R., Tokunaga, E., Ohmori, H., and Hirano, M., eds., Concepts and Modelling in Geomorphology: International Perspectives: Terrapub Publishers, Tokyo, p.199-220.

[10] Guth, P.L., 2001, Quantifying terrain fabric in digital elevation models, in Ehlen, J., and Harmon, R.S., eds., The environmental legacy of military operations, Geological Society of America Reviews in Engineering Geology , vol. 14, p.13-25.

[11] Hilley, G. E., S. DeLong, C. Prentice, K. Blisniuk, and JR Arrowsmith, 2010 "Morphologic Dating of Fault Scarps using Airborne Laser Swath Mapping (ALSM) Data." Geophysical Research Letters, vol. 37, no. 4, L04301, doi:10.1029/2009GL042044.